AIP | Applied Physics Letters

Local potential fluctuation of topological surface states in Bi1.5Sb0.5Te1.7Se1.3 observed by Landau level spectroscopy

Wonhee Ko, Joonbum Park, Insu Jeon, Hyo Won Kim, Hyeokshin Kwon, Youngtek Oh, Jun Sung Kim, Hwansoo Suh, Sung Woo Hwang, and Chilhee Chung

Citation: Applied Physics Letters **108**, 083109 (2016); doi: 10.1063/1.4942517
View online: http://dx.doi.org/10.1063/1.4942517
View Table of Contents: http://scitation.aip.org/content/aip/journal/apl/108/8?ver=pdfcov
Published by the AIP Publishing

Local potential fluctuation of topological surface states in $Bi_{1.5}Sb_{0.5}Te_{1.7}Se_{1.3}$ observed by Landau level spectroscopy

Wonhee Ko,[1,a)] Joonbum Park,[2] Insu Jeon,[1] Hyo Won Kim,[1] Hyeokshin Kwon,[1] Youngtek Oh,[1] Jun Sung Kim,[2] Hwansoo Suh,[1,a)] Sung Woo Hwang,[1] and Chilhee Chung[1]
[1]*Device Laboratory, Samsung Advanced Institute of Technology, Suwon 443-803, South Korea*
[2]*Department of Physics, Pohang University of Science of Technology, Pohang 790-784, South Korea*

(Received 1 October 2015; accepted 10 February 2016; published online 23 February 2016)

We report the local observation of the band structure of topological surface states in $Bi_{1.5}Sb_{0.5}Te_{1.7}Se_{1.3}$ using scanning tunneling microscopy/spectroscopy (STM/STS). The energy-momentum dispersion relation is locally deduced by extracting the Landau level (LL) energies, which are formed in a high magnetic field, from the STS data. Spatial variation of LLs revealed a shift of the Dirac point energy at the nanometer scale. The structure of the potential fluctuation was not correlated with the topography, which indicated that the Te/Se substitution did not induce the potential shift because of their same valence. The results show that disorders from the Te/Se substitution at the surface do not induce any localized charged states and do not affect topological surface states. © *2016 AIP Publishing LLC*. [http://dx.doi.org/10.1063/1.4942517]

Controlling doping in topological insulators is crucial both for achieving the potential of topological surface states by making their bulk insulating[1,2] and for utilizing their properties in novel device applications.[3] Various methods for doping topological insulators have been investigated, such as adding impurities[4] and applying external field by gating.[5] In addition, recent studies showed that it is possible to induce doping by adjusting the composition in Bi- and Sb-based chalcogenides, i.e., varying the composition variables x and y in $Bi_{2-x}Sb_xTe_{3-y}Se_y$.[6,7] In these compounds, the Fermi energy could be located in the bulk band gap, while the topological surface states remained intact. The existence of topological surface states has been confirmed by various methods such as angle-resolved photoemission spectroscopy (ARPES),[6,8] scanning tunneling microscopy/spectroscopy (STM/STS),[8,9] and transport measurements.[2,7,10,11]

Because $Bi_{2-x}Sb_xTe_{3-y}Se_y$ is an alloy with each layer consisting of a random mixture of two different elements, disorders occur naturally. These disorders require significant consideration because of the expected deterioration of the electrical properties such as the electron mean free path and mobility.[2,7–9] Microscopically, disorders induce potential variation that results in charge puddles and increased electron scattering, which has been observed in many two-dimensional electron systems including topological insulators.[4,12–15] $Bi_{2-x}Sb_xTe_{3-y}Se_y$ should have large local composition variation due to its non-stoichiometric structure and local potential fluctuation as a result,[2,6,7] but microscopic observation of charge puddle formation and information on their structure are absent in this material, which are essential for understanding the effects of composition variation on surface states.

In this study, we utilized STM/STS in high magnetic fields to measure the Landau levels (LLs) formed in topological surface states (referred to as LL spectroscopy). Through the peak position and shape of the conductance spectra, LL spectroscopy provides information on various electronic properties such as the local chemical potential and electron coherence.[16–19] Among the various compositions of $Bi_{2-x}Sb_xTe_{3-y}Se_y$, we selected $Bi_{1.5}Sb_{0.5}Te_{1.7}Se_{1.3}$ (BSTS) for this study because of its superior electronic properties, resulting from the lowest bulk carrier density.[2,6,7,10] Topography of the cleaved surface exhibited a surface composed of Te and Se with atomic resolution.[9] Well-preserved topological surface states are confirmed from the LL energies following the dispersion of massless Dirac fermions. Combining LL spectroscopy with STM, the surface band dispersion could be measured with nanometer resolution, where the shift of the Dirac point energy was observed and the local potential fluctuation was quantified. The local potential had little correlation with the surface topography, which implied that the substitution between Te and Se atoms at the surface did not induce any local doping, which was expected from their same valence.[20] The results indicate that although $Bi_{2-x}Sb_xTe_{3-y}Se_y$ is a highly disordered non-stoichiometric material, disorders from the Te/Se substitution at the surface do not induce localized charge states.

Single crystals of $Bi_{1.5}Sb_{0.5}Te_{1.7}Se_{1.3}$ were grown using the self-flux method according to a previously reported recipe.[9,10] A Unisoku low-temperature STM was used for the STM/STS measurements. The sample was cleaved in an ultrahigh vacuum chamber ($\sim 10^{-10}$ Torr) at room temperature and then transferred to the low-temperature STM stage at 2.8 K. A conventional lock-in technique was used to measure the conductance spectrum with a modulation voltage of 3 mV and a modulation frequency of 739 Hz.

Figure 1(a) shows a topograph of BSTS with atomic resolution. The small corrugation in the topograph should be a result of alloying between Se and Te in the topmost layer, according to the height distribution of the atoms.[9,21] An example of conductance spectra g, which are acquired at single point on the surface and exhibited clearest difference for varying magnetic fields, are shown in Fig. 1(b).[21] At 0 T, the

[a)]Authors to whom correspondence should be addressed. Electronic addresses: wonhee12.ko@samsung.com and hwansoo.suh@samsung.com.

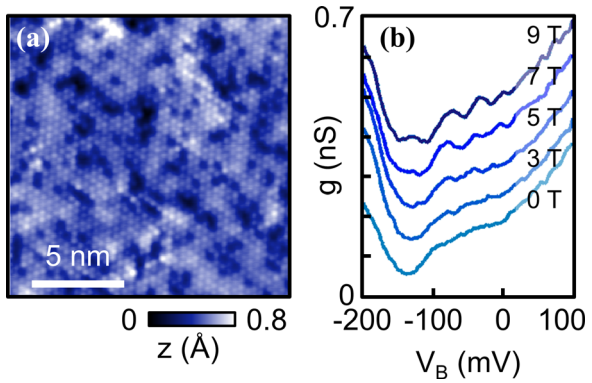

FIG. 1. (a) A topograph of the BSTS surface ($V_B = -400$ mV, $I = 0.2$ nA). (b) Conductance spectra acquired at one point in various magnetic fields. Each spectrum is vertically displaced for clarity.

spectrum resembles the typical spectra of Bi chalcogenides,[4,16,22] and as the magnetic field increases, several peaks appear; the spacing of these peaks increases with the magnetic field. Such peaks indicate the presence of two-dimensional surface states and their quantization in the field by the formation of LLs.[16–18,23] Other possibilities for the observed maxima in the spectra, such as the first resonance of standing waves in between the defects like in Morgenstern *et al.*,[24] are excluded because the inter-defect spacing is much smaller than the wavelength of the electrons.

Precise LL peak positions V_n were extracted by plotting the subtracted conductance spectrum Δg, which is calculated by subtracting the 0-T spectrum from the other spectra (Fig. 2(a)). Following the method by Hanaguri *et al.*,[17] we extracted the surface band dispersion by calculating the energy and momentum as $E_n = eV_n$ and $k_n = \sqrt{(2e\hbar|n|B)}$ and fitting these values to the dispersion of massless Dirac fermions

$$E_n = E_D + v_F\hbar k_n - D(\hbar k_n)^2,$$

where E_D is the Dirac point energy, v_F is the Fermi velocity, D is the second-order coefficient, e is the electron charge, $\hbar$ is the Planck constant divided by 2π, n is the LL index, and B is the magnitude of the magnetic field. In the equation, band is assumed to be isotropic and second-order term is added to account for the band curvature of topological surface states.[25] Among the various possible indexing of LLs, we chose the index that assigns $n = 0$ to the peak at about -80 meV for the following reasons. First, the peak at about -80 meV appears in the point spectra for all magnetic fields. Second, the residual of the fit is minimized for such indexing. Lastly, the extracted values of $E_D = -81$ meV and $v_F = 3.2 \times 10^5$ m/s match previously reported values.[6,8,9,21] We note that the Dirac point E_D extracted from the zeroth LL is higher than the minimum point of the conductance, which is not conventional compared to other Bi chalcogenides.[4,22] The reason for this difference is unknown, but one speculation is that bulk of BSTS might have an unusual band structure from alloying, where a significant amount of local potential fluctuation and defect states should exist. Moreover, we note that additional peak appears below -80 meV, which is marked by n*. However, the peak energy significantly deviates from the surface band dispersion, so we speculate that the peak may originate from the bulk valence band or the surface band hybridized with the bulk band.

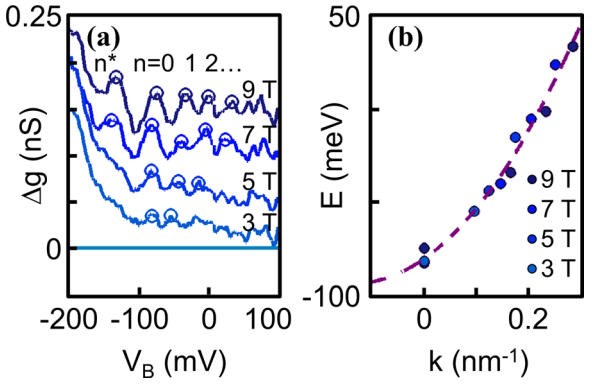

FIG. 2. (a) Subtracted conductance spectra, where the 0-T spectrum is subtracted from all other spectra in Fig. 1(b). Circles mark the peaks extracted from the spectra. Each spectrum is vertically displaced for clarity. (b) Energy plotted with respect to the wavevector, where the wavevectors are calculated assuming $n = 0$ for peaks at $V_B \sim -80$ mV. The fit to the Dirac band dispersion is drawn with a dashed line.

The LL peaks at different locations exhibited variation in energy, which indicated variation in the local potential.[12,14,19] To acquire a detailed view of the LL variation in space, a complete mapping of LLs over the area in Fig. 3(a) was achieved by acquiring the conductance spectra on equally spaced grid points at 0 T and 9 T. Figure 3(b) shows the selected conductance spectra acquired at five different points in Fig. 3(a). Both the 0-T and 9-T spectra show fluctuation of the Dirac point energy E_D, which is revealed by the shifts of the minimum point in 0 T and the zeroth LL peak position in 9 T. In Fig. 3(c), the subtracted conductance spectra between 0 T and 9 T are plotted, and the shift of zeroth LL peaks is shown more clearly (black arrows). In Figs. 3(d) and 3(e), the conductance spectra are rearranged and plotted as a spatial map at each bias voltage. Both the 0-T and 9-T conductance maps show similar patterns of bright and dark regions (Figs. 3(d) and 3(e), respectively), whose contrast is reversed when the bias is changed from -130 mV to -45 mV (most evidently at the lower left and the lower right regions). Such contrast inversion, which occurs when the bias crosses the Dirac point, indicates that the contrast originates from the Dirac point fluctuation, where the brighter spot at the bias above the Dirac point corresponds to a more negative Dirac point at that position.[15] Similarity between the maps at 0 T and 9 T indicates that the contrast is dominated by the Dirac point fluctuation even at high magnetic fields. However, when we subtract the maps at 0 T and 9 T, a subtle difference from the development of LLs appears (Fig. 3(f)). Because LLs appear as peaks in the subtracted conductance spectra, the maps show a higher signal when the bias coincides with the local LL energies, especially for the zeroth LL. Indeed, the subtracted conductance maps show an enhanced signal around the corresponding location, such as the lower left corner at $V_B = -45$ mV, the lower right corner at $V_B = -25$ mV, and the upper right corner at $V_B = -5$ mV. In contrast, when the bias is far from the Dirac point so that

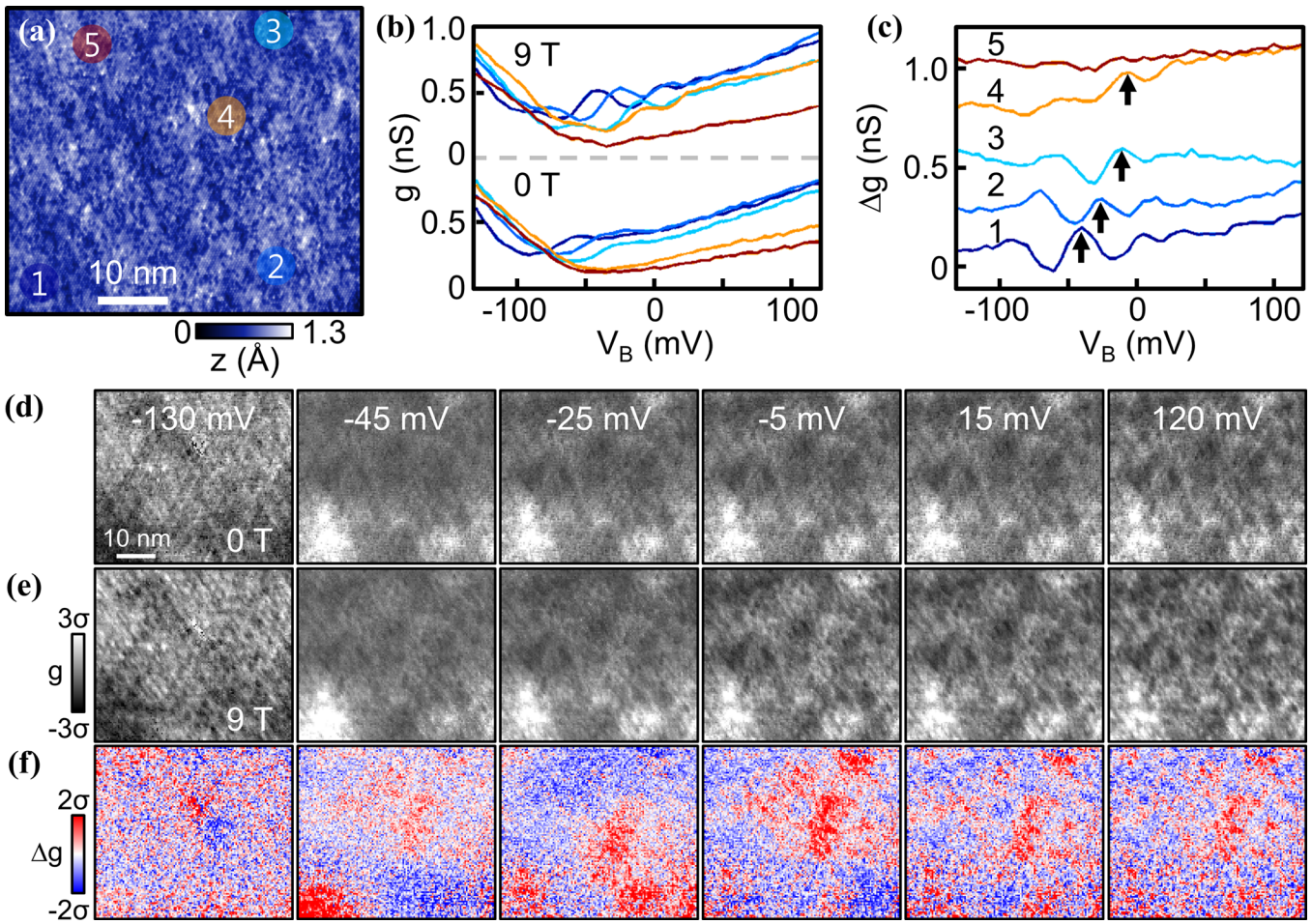

FIG. 3. (a) A topograph of the area where the conductance maps are acquired ($V_B = -300$ mV, $I = 0.2$ nA). (b) Conductance spectra at various positions marked by numbered dots in magnetic fields of 0 T and 9 T. The line color of the spectra corresponds to the color of the dots in (a). (c) Subtracted conductance spectra from (b). Note that each spectrum is vertically displaced for clarity in (c), but not in (b). (d) and (e) Conductance maps in the magnetic fields of 0 T and 9 T over the region in (a). (f) Subtracted conductance maps between 0 T and 9 T. In (d)–(f), color scales are normalized so that the center of the color distribution is a mean and the range is a multiple of the standard deviation σ of each map.

LLs are no longer resolved in the conductance spectra, such as $V_B = -130$ and 120 mV, the maps are quite uniform except for the speckle noise. The puddle size can be inferred from the size of the strong signal spots in the subtracted conductance maps. The smallest puddle size is about 10 nm, whose comparison with the magnetic length $l_B = [\hbar/(|e|B)]^{1/2}$ shows that they become identical at around $B = 7$ T. The LLs should appear clearly as the field reaches that value, which is consistent with our observation in Fig. 1(b).

In addition to the qualitative analysis, we extracted LL energies and band parameters from the conductance maps in Fig. 3 and characterized their spatial variation quantitatively. The LL maps for $n = 0$, 1, and 2 are plotted in Figs. 4(a)–4(c). All LL maps show positive correlation with each other, indicating that they are LLs shifted by the potential variation. Especially, Dirac point energy E_D is equal to E_0, so Fig. 4(a) is also the map of E_D whose variation corresponds to the quantitative representation of the local potential fluctuation and resulting charge puddles.[12,18,19] Figure 4(d) shows the map of v_F calculated from the LL energies as $v_F = (E_1 - E_0)/\sqrt{(2e\hbar B)}$ (the second-order term in the dispersion is neglected because E_n for $n > 1$ are difficult to extract due to their small amplitude, and its effect in v_F is small). The map of v_F in Fig. 4(d) shows that the values reside

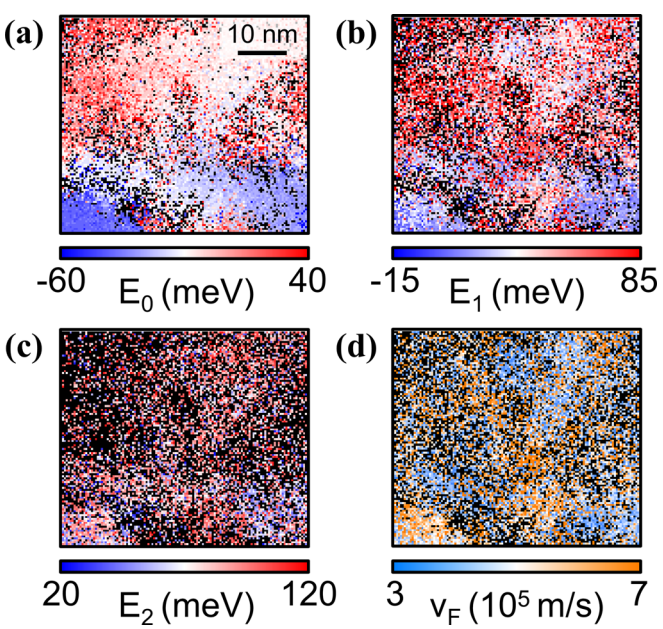

FIG. 4. (a)–(c) The LL maps for $n = 0$, 1, 2, respectively. (d) Fermi velocity, v_F. In all maps, the points in which the corresponding quantity is not extractable are black.

mostly in the range of $3–5 \times 10^5$ m/s, while there are some fluctuations. At this point, we are unsure if the fluctuation in v_F is from the noise caused by the small amplitude of high-index LL peaks[21] or by a physical origin such as the effect from the local charge states.[26] The error estimation from the zeroth LL peak width $\Delta \approx 20$ meV shows that the measured fluctuation in E_D from -60 to 40 meV is much larger than Δ, while the fluctuation in v_F is comparable to the expected error of $\Delta/\sqrt{(2e\hbar B)} \sim 2 \times 10^5$ m/s. Although the exact determination would require the measurement at higher magnetic fields with increased LL amplitude and energy spacing, we note that local potential fluctuation should only shift the position of Fermi level, not the slope of band dispersion,[4] and it is more likely that the spatial variation of v_F is coming from the measurement error.

One important question for BSTS is whether the alloying between Bi (Te) and Sb (Se) induces local potential fluctuation. The correlation between the map of E_D and the topography was estimated by calculating correlation coefficient R as

$$R = \frac{\sum_{x,y}\left(A_{xy} - \bar{A}\right)\left(B_{xy} - \bar{B}\right)}{\sqrt{\left(\sum_{x,y}\left(A_{xy} - \bar{A}\right)^2\right)\left(\sum_{x,y}\left(B_{xy} - \bar{B}\right)^2\right)}},$$

where A and B are the maps of physical quantities. However, due to the large difference in the length scale of the map of E_D ($\sim$10 nm) and the topograph ($\sim$1 nm), direct calculation of R would underestimate it because the feature of the map with smaller length scale will oscillate a lot in the feature of the map with the larger. To compensate the length scale difference, we first calculated correlation length ξ with autocorrelation analysis, where $\xi_{ED} = 6.9 \pm 0.2$ nm and $\xi_{topo} = 1.6 \pm 0.2$ nm.[21] Then, we increased ξ_{topo} by low pass filtering and calculated R between the filtered topograph and the map of E_D. For all ξ_{topo}, R was always smaller than 0.35, which is too small to derive any correlation between the local potential and the topography. The result agrees with the expectation that the substitution between Te and Se would not generate any additional charge states due to their same valence. Exact determination of the origin of the local potential fluctuation would require further investigation, such as the comparison between $Bi_{2-x}Sb_xTe_{3-y}Se_y$ with different compositions[6,7] or observations over well-defined chalcogenide heterostructures.[27]

In summary, the band structure of the topological surface states in BSTS has been observed locally through LL spectroscopy with STM/STS. The Dirac point energy showed significant spatial variation induced by local potential fluctuation, while the variation of the Fermi velocity was comparable to the measurement error. Comparison between the local potential and topography indicated that the local potential is not related to the local atomic composition at the surface, which implies that the Te/Se substitution at the topmost surface did not generate any localized charge states. Further study may reveal the exact mechanism of the doping, which would become a guide for growing topological insulators with the most optimal and homogenous doping that would be essential for realizing topological devices.[28]

The authors would like to acknowledge helpful discussions with Se-Jong Kahng and JiYeon Ku.

[1]J. G. Analytis, R. D. McDonald, S. C. Riggs, J. H. Chu, G. S. Boebinger, and I. R. Fisher, Nat. Phys. **6**(12), 960 (2010).
[2]Y. Xu, I. Miotkowski, C. Liu, J. Tian, H. Nam, N. Alidoust, J. Hu, C. K. Shih, M. Z. Hasan, and Y. P. Chen, Nat. Phys. **10**(12), 956 (2014).
[3]L. Fu and C. L. Kane, Phys. Rev. Lett. **100**(9), 096407 (2008); X. L. Qi, R. Li, J. Zang, and S. C. Zhang, Science **323**(5918), 1184 (2009).
[4]H. Beidenkopf, P. Roushan, J. Seo, L. Gorman, I. Drozdov, Y. S. Hor, R. J. Cava, and A. Yazdani, Nat. Phys. **7**(12), 939 (2011).
[5]T. Zhang, J. Ha, N. Levy, Y. Kuk, and J. Stroscio, Phys. Rev. Lett. **111**(5), 056803 (2013).
[6]T. Arakane, T. Sato, S. Souma, K. Kosaka, K. Nakayama, M. Komatsu, T. Takahashi, Z. Ren, K. Segawa, and Y. Ando, Nat. Commun. **3**, 636 (2012).
[7]Z. Ren, A. A. Taskin, S. Sasaki, K. Segawa, and Y. Ando, Phys. Rev. B **84**(16), 165311 (2011).
[8]S. Kim, S. Yoshizawa, Y. Ishida, K. Eto, K. Segawa, Y. Ando, S. Shin, and F. Komori, Phys. Rev. Lett. **112**(13), 136802 (2014).
[9]W. Ko, I. Jeon, H. W. Kim, H. Kwon, S. J. Kahng, J. Park, J. S. Kim, S. W. Hwang, and H. Suh, Sci. Rep. **3**, 2656 (2013).
[10]J. Lee, J. Park, J. H. Lee, J. S. Kim, and H. J. Lee, Phys. Rev. B **86**(24), 245321 (2012).
[11]K. Segawa, Z. Ren, S. Sasaki, T. Tsuda, S. Kuwabata, and Y. Ando, Phys. Rev. B **86**(7), 075306 (2012); A. A. Taskin, Z. Ren, S. Sasaki, K. Segawa, and Y. Ando, Phys. Rev. Lett. **107**(1), 016801 (2011); Z. Ren, A. A. Taskin, S. Sasaki, K. Segawa, and Y. Ando, Phys. Rev. B **82**(24), 241306 (2010).
[12]Y. Niimi, H. Kambara, T. Matsui, D. Yoshioka, and H. Fukuyama, Phys. Rev. Lett. **97**(23), 236804 (2006).
[13]J. Martin, N. Akerman, G. Ulbricht, T. Lohmann, J. H. Smet, K. Von Klitzing, and A. Yacoby, Nat. Phys. **4**(2), 144 (2008).
[14]M. Morgenstern, Chr. Wittneven, R. Dombrowski, and R. Wiesendanger, Phys. Rev. Lett. **84**(24), 5588 (2000).
[15]C. Mann, D. West, I. Miotkowski, Y. P. Chen, S. Zhang, and C. K. Shih, Nat. Commun. **4**, 2277 (2013).
[16]P. Cheng, C. Song, T. Zhang, Y. Zhang, Y. Wang, J. F. Jia, J. Wang, Y. Wang, B. F. Zhu, X. Chen, X. Ma, K. He, L. Wang, X. Dai, Z. Fang, X. Xie, X. L. Qi, C. X. Liu, S. C. Zhang, and Q. K. Xue, Phys. Rev. Lett. **105**(7), 076801 (2010).
[17]T. Hanaguri, K. Igarashi, M. Kawamura, H. Takagi, and T. Sasagawa, Phys. Rev. B **82**(8), 081305 (2010).
[18]Y. Okada, W. Zhou, C. Dhital, D. Walkup, Y. Ran, Z. Wang, S. D. Wilson, and V. Madhavan, Phys. Rev. Lett. **109**(16), 166407 (2012).
[19]Y. S. Fu, M. Kawamura, K. Igarashi, H. Takagi, T. Hanaguri, and T. Sasagawa, Nat. Phys. **10**(11), 815 (2014).
[20]R. J. Cava, H. Ji, M. K. Fuccillo, Q. D. Gibson, and Y. S. Hor, J. Mater. Chem. C **1**(19), 3176 (2013).
[21]See supplementary material at http://dx.doi.org/10.1063/1.4942517 for the details of analysis on the maps and their correlations.
[22]Z. Alpichshev, J. G. Analytis, J. H. Chu, I. R. Fisher, Y. L. Chen, Z. X. Shen, A. Fang, and A. Kapitulnik, Phys. Rev. Lett. **104**(1), 016401 (2010).
[23]Y. S. Fu, T. Hanaguri, S. Yamamoto, K. Igarashi, H. Takagi, and T. Sasagawa, ACS Nano **7**(5), 4105 (2013); Y. Jiang, Y. Wang, M. Chen, Z. Li, C. Song, K. He, L. Wang, X. Chen, X. Ma, and Q. K. Xue, Phys. Rev. Lett. **108**(1), 016401 (2012).
[24]K. Morgenstern, K. F. Braun, and K. H. Rieder, Phys. Rev. Lett. **89**(22), 226801 (2002).
[25]M. H. Berntsen, O. Götberg, B. M. Wojek, and O. Tjernberg, Phys. Rev. B **88**(19), 195132 (2013); H. Z. Lu, W. Y. Shan, W. Yao, Q. Niu, and S. Q. Shen, *ibid.* **81**(11), 115407 (2010); A. A. Taskin and Y. Ando, *ibid.* **84**(3), 035301 (2011).
[26]A. Luican-Mayer, M. Kharitonov, G. Li, C. P. Lu, I. Skachko, A. M. B. Gonçalves, K. Watanabe, T. Taniguchi, and E. Y. Andrei, Phys. Rev. Lett. **112**(3), 036804 (2014).
[27]Q. Zhang, Z. Zhang, Z. Zhu, U. Schwingenschlögl, and Y. Cui, ACS Nano **6**(3), 2345 (2012); T. V. Menshchikova, M. M. Otrokov, S. S. Tsirkin, D. A. Samorokov, V. V. Bebneva, A. Ernst, V. M. Kuznetsov, and E. V. Chulkov, Nano Lett. **13**(12), 6064 (2013); G. Wu, H. Chen, Y. Sun, X. Li, P. Cui, C. Franchini, J. Wang, X. Q. Chen, and Z. Zhang, Sci. Rep. **3**, 1233 (2013).
[28]Y. Shiomi, K. Nomura, Y. Kajiwara, K. Eto, M. Novak, K. Segawa, Y. Ando, and E. Saitoh, Phys. Rev. Lett. **113**(19), 196601 (2014); C. H. Li, O. M. J. Van't Erve, J. T. Robinson, Y. Liu, L. Li, and B. T. Jonker, Nat. Nanotechnol. **9**(3), 218 (2014).